

3D in vitro neuron on a chip for probing calcium mechanostimulation

Justin Bobo*, Akash Garg, Prahatha Venkatraman, Manoj Puthenveedu, and Philip R. LeDuc*

((Optional Dedication))

J. Bobo, A. Garg, Prof. P. R. LeDuc

Department of Mechanical Engineering, Carnegie Mellon University, 5000 Forbes Ave, Pittsburgh, Pennsylvania, 15213, USA

E-mail: jbobob@andrew.cmu.edu, prl@andrew.cmu.edu

Prof. P. R. LeDuc

Department of Biological Sciences, Carnegie Mellon University, 5000 Forbes Ave, Pittsburgh, Pennsylvania, 15213, USA

Dr. P. Venkatraman, Prof. M. Puthenveedu

Department of Pharmacology, University of Michigan, 1150 W Medical Center Dr, Ann Arbor, MI 48109, USA

Keywords: mechanostimulation, tissue on a chip, micro-scale, calcium

Abstract

The evolution of tissue on a chip systems holds promise for mimicking the response of biological functionality of physiological systems. One important direction for tissue on a chip approaches are neuron based systems that could mimic neurological responses and lessen the need for *in vivo* experimentation. For neural research, more attention has been devoted recently to understanding

This is the author manuscript accepted for publication and has undergone full peer review but has not been through the copyediting, typesetting, pagination and proofreading process, which may lead to differences between this version and the [Version of Record](#). Please cite this article as [doi: 10.1002/adbi.202000080](#).

mechanics due to issues in areas such as traumatic brain injury and pain, among others. To begin to address these areas, we developed a 3D Nerve Integrated Tissue on a Chip approach combined with a Mechanical Excitation Testbed System to impose external mechanical stimulation toward more realistic physiological environments. We used PC12 cells differentiated with nerve growth factor, which were cultured in our controlled 3D scaffolds. We labelled the cells with Fluo-4-AM to examine their calcium response under mechanical stimulation. We imposed mechanical stimulation synchronized with image capturing to examine the cellular response in our 3D nerve integrated tissue on a chip system. Understanding the neural responses to mechanical stimulation beyond 2D systems is very important for neurological studies and future personalized strategies. We feel that this work will have implications in a diversity of areas including tissue on a chip systems, biomaterials, and neuromechanics.

1. Introduction

3D tissue on a chip systems are considered promising candidates for a variety of fields including tissue engineering, organ regeneration, and *in vitro* disease models.^[1-4] These multi-dimensional systems at a miniaturized scale seek to mimic physiology without using animals or humans. In these systems, 3D cell-to-cell interactions form potentially providing new *in vitro* approaches to study and mimic the response of biological and cellular processes. One particularly interesting area to study is mechanical stimulation due to its importance in a wide range of physiological systems from cardiac to neural areas. In the neural domain, previous approaches for examining the effects of *in vitro* mechanical loading on cells have focused mostly on local stimulation of single or multiple neurons cultured on planar substrates. These approaches have proven to be useful for understanding how mechanical stimuli are transduced to biochemical signals including being integrated with micro-fabricated environments.^[5-8] While much of the knowledge of cellular biomechanics focuses on our understanding from planar substrates, these 2D systems unfortunately lack physiological aspects

such as three dimensionality as well as the complexity of tissue and neuronal function. 3D culture systems can enhance the analysis of integrated interactions between tissue and neural response to recapitulate the natural microenvironment with spatiotemporal details, which may be relevant in understanding many issues including Alzheimer's disease and traumatic brain injury (TBI).^[9-11]

This type of understanding of biomechanics is particularly important as TBI can result from a diversity of situations such as a car crash, an innocuous fall, sports injury, and sudden jolts or blows to the head. Annually these types of issues affect approximately 1.5 million people in the United States and 69 million individuals worldwide as well as accounting for 1/3 of all injury-related deaths in the United States affecting every stage of life from adolescents to the elderly.^[12,13] Precisely identifying the importance of dysfunction and pathomorphological expressions after external mechanical insult is very important. These responses include a variety of factors such as compressive strains and subcellular responses. The approaches with tissue on a chip systems could help in these areas as representative building blocks for assessing *in vitro*, multi-dimensional organ architectures toward physiological understanding and treatment.

Understanding cell responses under mechanical stimulation can be probed through many techniques. One approach involves an important molecular signature related to mechanostimulation of calcium (Ca^{2+}) signaling. Ca^{2+} is an ubiquitous second messenger participating in signal transduction in cells throughout the body and is known to have roles in vital processes such as fertilization, muscle contraction, growth and development, neural transmission, and gene expression.^[14-16] Ca^{2+} also plays a key role in the release of synaptic vesicles when a neuron fires, but this could lead to damage and cell death under an overload of the mitochondria and intense activation of Ca^{2+} dependent enzymes. Altered Ca^{2+} ion homeostasis is also linked to several

This article is protected by copyright. All rights reserved.

neurodegenerative diseases: Parkinson's, Huntington's, Alzheimer's, amyotrophic lateral sclerosis, and TBI.^[17-21] Although previous 2D studies of Ca^{2+} conducted *in vitro* examined Ca^{2+} concentrations related to stretch^[22], a complete understanding of neuronal functionality in a three-dimensional platform combined with spatiotemporal detail, would provide tremendous insight to neuromechanical responses and potential treatments in the future.

Here, we developed a 3D collagen Nerve Integrated Tissue on Chip (NITC) system to mimic tissue engineering physiology. We then imposed mechanical stimulation on the NITC and examined Ca^{2+} responses under dynamic loading. Given the importance of compressive deformation to neurotrauma and impact injuries with understanding their long term effects, we believe that our approach will provide new knowledge in areas including neuromechanics, biomaterials, and 3D cellular response.

2. Results and Discussion

2.1. 3D Cellular Collagen Scaffolds Under Mechanical Stimulation

To study Ca^{2+} response in NGF induced PC12 cells, Fluo-4-AM (stock: 50 μg , molecular weight: 1097 g/mole), which is a cell permeant Ca^{2+} indicator, was introduced to the cells. Fluo-4-AM was pipetted onto the NGF induced PC12 cells, which were then incubated for 1 h.^[23-24] Ca^{2+} stained cells were added to 10X phosphate buffered saline (PBS), sodium hydroxide (NaOH), and type 1 collagen to form a cross-linked ECM. Collagen type I, which is the most abundant protein found in mammals as well as being naturally present in many 3D matrices in various tissues, was used as the ECM.^[25,26] The collagen concentration with embedded PC12 cells was 5 mg/mL, which allowed us to maintain structural stability while applying external mechanical, compressive loading. This concentration is

slightly higher than *in vivo* ECMs, however, this is in a physiologically relevant concentration range and also maintains its structural stability, which is essential in mechanical testing.^[27]

We developed a direct and reproducible method to cast the cross-linked PC12 collagen scaffolds.

Molds were created to encapsulate the 3D NITC systems by mounting a circular acrylic ring (12mm ID/15 mm OD) to a 25 mm coverslip using Norland 85 biocompatible glue to enable a clear path for imaging and housing of the PC12 collagen scaffolds (**Figure 1B**). After loading the cells into collagen on acrylic ringed coverslips, spinning disk confocal microscopy imaging was done to examine the NGF induced PC12 cells. The cells displayed a distinct green fluorescence signal with a 3:1000 dilution factor (2 mL F-12K Medium, 6 μ L of diluted Fluo-4-AM dye) from the Fluo-4-AM loaded NGF induced PC12 cells (**Figure 1C**). Additional information on cell-culture, live-cell fluorescent imaging, and techniques to analyze a multi-dimensional ECM are in the Experimental Section and Supplemental Materials (SI Tab. T1).

2.2. 3D Cellular Collagen Scaffolds Under Mechanical Stimulation

One promising approach for applying systematic mechanics is our Mechanical Excitation Testbed (MET) that implements a voice coil actuator to impose different modes of fast mechanical stimulation including single stimulation excitation (s-stim) and repetitive stimulation (r-stim) excitation onto 3D collagen scaffolds. We designed our approach so that we apply mechanical stimuli that would mimic different degrees of important neuromechanics occurring in more physiologically relevant areas. One of these areas that we mimic is head injuries, as the degree of injury severity is distinguished as mild, moderate, or severe, and consists of primary and secondary phases.^[28,29] The primary phase is the initial point of active mechanical stimulation while the secondary phase is the period post stimulation. During the primary phase, the force transduced is largely compressive from the initial impact-derived deformation.^[30-33] With our approach using the

MET system, we can apply controllable and tunable compression to our cellularized 3D biomaterial, collagen gels, to mimic degrees of injury severity under mechanical stimulation on our 3D models.

The MET system (Figure 2, SI Equation 1-4) applies systematic uniaxial rectilinear compressive motion to the cellularized collagen gels by modulating a linear voice coil (VCA) (HVCM-016-010-003-01; Moticont, Van Nuys, CA 91406) housed inside a custom (Solidworks Corp., 2018) 3D printed (Object350) housing with a precision force applicator arm (named “end effector”). The custom 3D printed stand is connected to a linear stage (4053 Parker Daedal Ball Bearing Positioner) used for precise positioning of the force applicator arm. The incorporation of a VCA allows for controllable and tunable actuation through the position interval displacement as a function of time. The VCA is powered and controlled using a function generator and a custom printed electronic circuit board (PCB) (EAGLE, AutoDesk) (Figure 2C, SI Figure S1). To account for the inherent noise from the VCA, an operational amplifier (OPA544T) was designed into the PCB. The PCB board combined component placement and routing layouts to control electrical connectivity. Current flows from the op-amp PCB board to the VCA in a feedback loop.

The MET generates controlled displacement waveforms (Figure 2A) over a wide range of frequencies to simulate mild to severe external mechanical loading based on previous cellular TBI investigations, which applied strain rates that span 10^{-4} s^{-1} to 75 s^{-1} .^{11,34} Tuning the frequency, amplitude, and waveform changes the dynamic movement of the VCA from lower strain rate quasistatic motion loading to high strain rate dynamic motion loading. The studies presented here are all conducted using a sine waveform and model repeated applied strains.

Gathering information in real time is important for understanding the response of cells during different phases of stimulation. One challenge with using tissue on a chip systems with 3D *in vitro* gels is viewing changes such as movement of the system, which occurs with mechanical stimulation, using standard epifluorescence microscopy. Even more complicated is that 3D gels have cells in different planes and not just in a singular plane as is found in most 2D cell culture systems. To accommodate this, the MET device contains a structural support which mounts to the manual two axis stage directly in line with a spinning disk confocal microscope for controlled imaging. Combining the MET system with a high powered objective yields a working distance that can facilitate imaging of cells in different planes (Figure 1C). Our setup is also able to examine cells through the different z planes after the cellularized collagen gel is displaced by the precision end effector. Through capturing images during the entire mechanical stimulation, our approach is able to examine cells during each cycle as the cells return to the plane where the microscope is focused.

2.3. Analysis of Ca²⁺ labelled differentiated PC12 cells during mechanical excitation

To study the *in vitro* Ca²⁺ response for differentiated PC12 cells in 3D collagen scaffolds when stimulated by MET, precise imaging of the response over time was essential (**Figure 3**). To capture images, a 1 Hz frequency for the VCA was used through the function generator while applying controlled systematic amplitudes of strains to the gels. This approach allowed the ability to select a focal plane with cells in focus and then to stimulate the cells while capturing images. The experimental testing included a 60 s no-contact control phase, 60 s r-stim sine wave primary phase, and a 60 s secondary phase while imaging the Ca²⁺ labelled differentiated PC12 cells in collagen scaffolds (**Figure 4**).

The fluorescence response of the differentiated PC12 cell gels changes over time for each strain rate as observed in the distinct changes beginning at the primary phase. The first change within the NITC system was the immediate increase in intensity of Ca^{2+} (Figure 3: Primary Phase, 4B,4C, SI Vid. 1, S2, S3). Images during the no-contact control phase remained at steady state over the entire 60 s span for all 6 samples and pixel intensity was measured as an absolute maximum of Ca^{2+} (Figure 4A and 4D). Through analyzing the effects over time on the spatiotemporal distributions of Ca^{2+} , strain rate appears to have a distinct effect on Ca^{2+} in the neurons (Figure 4). For the two impact loading rates ($4 \times 10^{-2} \text{ s}^{-1}$ and $8 \times 10^{-2} \text{ s}^{-1}$), the primary phase had a significant difference in both peak maximum intensity and peak mean expression levels experienced by the 3D embedded cells (Figure 4D, 4E, 4F, 4G). We analyzed fluorescent cell response (Figure 4A-4C), which showed distinct changes after mechanical loading. An immediate increase with external mechanical excitation occurred in all of the samples regardless of the applied strain rate in the primary phase (Figure 4B, 4E, 4G,S2,S3). The red and blue data points of the primary phase (Figure 4E) are the recorded relative maximum Ca^{2+} intensity during each frame of time corresponding to cells going in and out of focus (Figure S3). For $E=4 \times 10^{-2} \text{ s}^{-1}$, we observed a Ca^{2+} increase of 9.74% and 17.3% for $E=8 \times 10^{-2} \text{ s}^{-1}$ (Figure 4G) which can be visually shown in the images of each phase (Figure 4A-4C). The distribution of pixel intensity as a relation to strain rate is greater during the primary phase resulting in a higher mean Ca^{2+} intensity (Figure 4G). The mechanically induced elevation in Ca^{2+} was not sustained following the primary phase and immediately began to decline in all tests (Figure 4G). During the secondary phase, the maximum Ca^{2+} intensity signal fluctuated during the 60 s window. This finding might be particularly important as altered Ca^{2+} homeostasis is linked to several neurodegenerative diseases including TBI.^[35-37] Our work has findings that align with others in the literature from a mechanics and Ca^{2+} perspective such as biomechanics and tissue deformations^[11,34,38-40] along with cellular Ca^{2+} levels.^[41-48] These previous papers show that after stretch and shear, cellular Ca^{2+} level exhibits comparable dynamic shifts to our reported work from 3D compressive loading. Rzigalinsk, et al reported

following stretch injury, Ca^{2+} is rapidly elevated proportional to the degree of injury.^[45] In the studies, Ca^{2+} elevation was not sustained after the stretch injury and returned to near-basal levels post injury. Maneshi, et al reported following shear stress increased Ca^{2+} depended on the magnitude, duration, and rise time of the stimulus^[46], which is aligned with our findings.

3. Conclusion

This study presents a 3D tissue on a chip neural system which examined cell response under mechanical stimulation. We designed a mimetic *in vitro* ECM collagen scaffold embedded with NGF induced PC12 cells and applied our MET system to assess spatiotemporal molecular response to external compressive stimulation. The creation of the MET device allowed us the flexibility for stimulation of the 3D tissue on a chip system by enabling systematic mechanical stimulation with live confocal imaging. With the ability to image the micro-environment under mechanical stimulation, new spatiotemporal details of *in vitro* Ca^{2+} responses during the No-Contact Control phase, Primary phase, and Secondary phase were found relative to strain rate. Given the frequency and prevalence of compressive loading during external mechanical impacts in different systems including to the head, the 3D *in vitro* findings of this study provide insight into the cell response relative to mechanical loading in an important area of Ca^{2+} signaling. This work could be a foundational building block to merging 3D *in vitro* multi-dimensional ECMs with architecture, bioactive, and mechanical cues to advance neuropathomorphology assessment. Future studies could also address variation of strain rates used to elicit biosensor response, ECM complexity, as well as machine learning based approaches to examine injury through *in vitro* based approaches.

4. Experimental Section/Methods

Cell Culture: PC12 cells (ATCC, CRL-1721TM) were cultured in F-12K Medium (Kaighn's Modification of Ham's F-12 Medium) (ATCC 30-2004TM) supplemented with 5% fetal bovine serum and 10% horse

This article is protected by copyright. All rights reserved.

serum. Cells were maintained in a humidified incubator held constant at 37 °C with ~5% CO₂. The collagen IV solution was prepared by mixing 5 mg of collagen IV and 5 mL of 0.25% acetic acid for 2 hours and coating the device overnight at 4 °C. Cells were plated in the collagen IV coated devices and allowed to grow to confluency following standard subculture protocol.^[49]

Fluorescent Ca²⁺ labeling and imaging with live cell capture: Fluo-4-AM (stock: 50 µg, molecular weight: 1097 g/mole), which is a cell permeant Ca²⁺ indicator, was diluted with DMSO as described by the ThermoFisher Scientific protocols. For 3D *in vitro* cellularized collagen scaffolds, 3:1000 dilution factor (2 mL F-12K Medium, 6 µL of diluted Fluo-4-AM dye) was used for Ca²⁺ labeling.^[50] PC12 cells with 50 ng/mL of NGF were incubated for 1 hour with Fluo-4-AM. Prior to Ca²⁺ imaging, Ca²⁺ stained cells were added to 10X PBS, NaOH, and type 1 collagen to form the cellularized ECM. The ECM was then allowed to cross-link for 1 hour before imaging. During mechanical stimulation, a spinning disk confocal microscope captured images at controlled speeds.

NITC device: To create an integrated 3D cellularized model tissue as an *in vitro* testing platform with mechanics, a biomaterials approach was combined with a mechanical testing approach (**Figure 1**). NITC devices were constructed with collagen 1 and 50 ng/mL Nerve Growth Factor (NGF) induced PC12 (ATCC, CRL-1721™) cells to promote neurite outgrowth. NGF induced PC12 cells were cultured in F-12K Medium (Kaighn's Modification of Ham's F-12 Medium) (ATCC 30-2004™) supplemented with 5% fetal bovine serum and 10% horse serum on collagen IV coated flasks. Cells were maintained in an incubator held constant at 37 °C with ~5% CO₂ with a medium change every 48 hours. Cells were allowed to grow to 80-90% confluency to an observable change in sympathetic neuron phenotype.

NITC device imaging: 3D NITC devices were plated on 25 mm coverslips surrounded by an acrylic ring chamber. The NITC device assembly was mounted on the stage of an inverted, spinning disk confocal microscope (Axio Observer Z1 Microscope System, Zeiss) with both a function generator (Agilent 33120A Function Generator) and a power supply (BK Precision 1760A Triple Output Power Supply). An oscilloscope (Rigol 100 MHz Digital) was also incorporated to verify the waveform of the signal with one for the signal of the function generator and another for the signal from the VCA. A custom printed circuit board using a high current, high voltage operational amplifier (OPA544T, Texas Instruments) was used to decrease the noise; the operational amplifier smoothed the signal from the VCA. Image capture was synchronized with the MET at a frequency of 1 Hz resulting in 180 images which were post-processed using python and NIH ImageJ software.

Statistical Analysis: Continuous variables are expressed as mean \pm SD. For all datasets, t-tests were conducted across all groups with significance defined as * $p \leq 0.05$ and ** $p \leq 0.01$. Statistical analysis was through NIH ImageJ and Microsoft Excel.

Supporting Information

Supporting Information is available from the Wiley Online Library or from the author.

Acknowledgements

This work was supported in part by the Air Force Office of Scientific Research (FA9550-18-1-0262), Office of Naval Research (N00014-17-1-2566), Pennsylvania Department of Health (SAP4100077084), and the National Institute of Health (R01AG06100501A1).

Received: ((will be filled in by the editorial staff))

Revised: ((will be filled in by the editorial staff))

Published online: ((will be filled in by the editorial staff))

References

- [1] Wagner, I., Materne, E.M., Brincker, S., Süßbier, U., Frädrich, C., Busek, M., Sonntag, F., Sakharov, D.A., Trushkin, E.V., Tonevitsky, A.G. and Lauster, R., 2013. A dynamic multi-organ-chip for long-term cultivation and substance testing proven by 3D human liver and skin tissue co-culture. *Lab on a Chip*, 13(18), pp.3538-3547.
- [2] Griffith, L.G. and Swartz, M.A., 2006. Capturing complex 3D tissue physiology in vitro. *Nature reviews Molecular cell biology*, 7(3), pp.211-224.
- [3] Wan, L., Skoko, J., Yu, J., Ozdoganlar, O.B., LeDuc, P.R. and Neumann, C.A., 2017. Mimicking embedded vasculature structure for 3D cancer on a chip approaches through micromilling. *Scientific Reports*, 7(1), pp.1-8.
- [4] Wan, L., LeDuc, P.R. and Neumann, C., 2017. 3D Vasculature Structure in Breast Cancer on a Chip Approaches through Micromilling. *The FASEB Journal*, 31(1_supplement), pp.942-1.
- [5] Ferrer, I., Blanco, R., Carmona, M., Puig, B., Barrachina, M., Gomez, C. and Ambrosio, S., 2001. Active, phosphorylation-dependent mitogen-activated protein kinase (MAPK/ERK), stress-activated protein kinase/c-Jun N-terminal kinase (SAPK/JNK), and p38 kinase expression in Parkinson's disease and Dementia with Lewy bodies. *Journal of neural transmission*, 108(12), pp.1383-1396.
- [6] Li, C., Hu, Y., Mayr, M. and Xu, Q., 1999. Cyclic strain stress-induced mitogen-activated protein kinase (MAPK) phosphatase 1 expression in vascular smooth muscle cells is regulated by Ras/Rac-MAPK pathways. *Journal of Biological Chemistry*, 274(36), pp.25273-25280.

This article is protected by copyright. All rights reserved.

- [7] Wang, Y., Botvinick, E.L., Zhao, Y., Berns, M.W., Usami, S., Tsien, R.Y. and Chien, S., 2005. Visualizing the mechanical activation of Src. *Nature*, 434(7036), pp.1040-1045.
- [8] Lin, Y.W., Cheng, C.M., LeDuc, P.R. and Chen, C.C., 2009. Understanding sensory nerve mechanotransduction through localized elastomeric matrix control. *PLoS One*, 4(1), p.e4293.
- [9] Zhang, D., Pekkanen-Mattila, M., Shahsavani, M., Falk, A., Teixeira, A.I. and Herland, A., 2014. A 3D Alzheimer's disease culture model and the induction of P21-activated kinase mediated sensing in iPSC derived neurons. *Biomaterials*, 35(5), pp.1420-1428.
- [10] Choi, S.H., Kim, Y.H., Hebisch, M., Sliwinski, C., Lee, S., D'Avanzo, C., Chen, H., Hooli, B., Asselin, C., Muffat, J. and Klee, J.B., 2014. A three-dimensional human neural cell culture model of Alzheimer's disease. *Nature*, 515(7526), pp.274-278.
- [11] Bar-Kochba, E., Scimone, M.T., Estrada, J.B. and Franck, C., 2016. Strain and rate-dependent neuronal injury in a 3D in vitro compression model of traumatic brain injury. *Scientific reports*, 6(1), pp.1-11.
- [12] "Report to Congress: Traumatic Brain Injury in the United States." *Centers for Disease Control and Prevention*, Centers for Disease Control and Prevention, 22 Jan. 2016, www.cdc.gov/traumaticbraininjury/pubs/tbi_report_to_congress.html.
- [13] Dewan, M.C., Rattani, A., Gupta, S., Baticulon, R.E., Hung, Y.C., Punchak, M., Agrawal, A., Adeleye, A.O., Shrinne, M.G., Rubiano, A.M. and Rosenfeld, J.V., 2018. Estimating the global incidence of traumatic brain injury. *Journal of neurosurgery*, 130(4), pp.1080-1097.
- [14] Augustine, G.J., Santamaria, F. and Tanaka, K., 2003. Local calcium signaling in neurons. *Neuron*, 40(2), pp.331-346.
- [15] Brown, E.M. and MacLeod, R.J., 2001. Extracellular calcium sensing and extracellular calcium signaling. *Physiological reviews*, 81(1), pp.239-297.

This article is protected by copyright. All rights reserved.

- [16] Clapham, D. E. "Calcium signaling." *Cell* 131.6 (2007): 1047-1058.
- [17] Mattson, M. P., LaFerla, F. M., Chan, S. L., Leissring, M. A., Shepel, P. N., and Geiger, J. D. (2000). Calcium signaling in the ER: its role in neuronal plasticity and neurodegenerative disorders. *Trends Neurosci.* 23, 222–229.
- [18] Heath, P. R., and Shaw, P. J. (2002). Update on the glutamatergic neurotransmitter system and the role of excitotoxicity in amyotrophic lateral sclerosis. *Muscle Nerve* 26, 438–458.
- [19] Nakamura, T., and Lipton, S. A. (2010). Preventing Ca²⁺-mediated nitrosative stress in neurodegenerative diseases: possible pharmacological strategies. *Cell Calcium* 47, 190–197.
- [20] Wojda, U., Salinska, E., and Kuznicki, J. (2008). Calcium ions in neuronal degeneration. *IUBMB Life* 60, 575–590.
- [21] Surmeier, D. J., Guzman, J. N., and Sanchez-Padilla, J. (2010). Calcium, cellular aging, and selective neuronal vulnerability in Parkinson's disease. *Cell Calcium* 47, 175–182.
- [22] Lusardi, T.A., Wolf, J.A., Putt, M.E., Smith, D.H. and Meaney, D.F., 2004. Effect of acute calcium influx after mechanical stretch injury in vitro on the viability of hippocampal neurons. *Journal of neurotrauma*, 21(1), pp.61-72.
- [23] Yang, Y.J., Lee, H.J., Choi, D.H., Huang, H.S., Lim, S.C. and Lee, M.K., 2008. Effect of scopolamine on neurite outgrowth in PC12 cells. *Neuroscience letters*, 440(1), pp.14-18.
- [24] Morabito, C., Guarnieri, S., Fanò, G. and Mariggiò, M.A., 2010. Effects of acute and chronic low frequency electromagnetic field exposure on PC12 cells during neuronal differentiation. *Cellular Physiology and Biochemistry*, 26(6), pp.947-958.
- [25] Cross, V.L., Zheng, Y., Choi, N.W., Verbridge, S.S., Sutermeister, B.A., Bonassar, L.J., Fischbach, C. and Stroock, A.D., 2010. Dense type I collagen matrices that support cellular remodeling and microfabrication for studies of tumor angiogenesis and vasculogenesis in vitro. *Biomaterials*, 31(33), pp.8596-8607.

- [26] Raub, C.B., Putnam, A.J., Tromberg, B.J. and George, S.C., 2010. Predicting bulk mechanical properties of cellularized collagen gels using multiphoton microscopy. *Acta biomaterialia*, 6(12), pp.4657-4665.
- [27] Artym, V.V. and Matsumoto, K., 2010. Imaging cells in three-dimensional collagen matrix. *Current protocols in cell biology*, 48(1), pp.10-18.
- [28] Brasure, M., Lamberty, G.J., Sayer, N.A., Nelson, N.W., MacDonald, R., Ouellette, J., Tacklind, J., Grove, M., Rutks, I.R., Butler, M.E. and Kane, R.L., 2012. Multidisciplinary postacute rehabilitation for moderate to severe traumatic brain injury in adults.
- [29] Kaur, P. and Sharma, S., 2018. Recent advances in pathophysiology of traumatic brain injury. *Current neuropharmacology*, 16(8), pp.1224-1238.
- [30] Nahum, A.M., Smith, R. and Ward, C.C., 1977. *Intracranial pressure dynamics during head impact* (No. 770922). SAE Technical Paper.
- [31] Kraft, R.H., Mckee, P.J., Dagro, A.M. and Grafton, S.T., 2012. Combining the finite element method with structural connectome-based analysis for modeling neurotrauma: connectome neurotrauma mechanics. *PLoS Comput Biol*, 8(8), p.e1002619.
- [32] Wright, R.M. and Ramesh, K.T., 2012. An axonal strain injury criterion for traumatic brain injury. *Biomechanics and modeling in mechanobiology*, 11(1-2), pp.245-260.
- [33] Young, L., Rule, G.T., Bocchieri, R.T., Walilko, T.J., Burns, J.M. and Ling, G., 2015. When physics meets biology: low and high-velocity penetration, blunt impact, and blast injuries to the brain. *Frontiers in neurology*, 6, p.89.
- [34] Pfister, B.J., Weihs, T.P., Betenbaugh, M. and Bao, G., 2003. An in vitro uniaxial stretch model for axonal injury. *Annals of biomedical engineering*, 31(5), pp.589-598.

- [35] Weber, J.T., 2012. Altered calcium signaling following traumatic brain injury. *Frontiers in pharmacology*, 3, p.60.
- [36] Kristián, T. and Siesjö, B.K., 1998. Calcium in ischemic cell death. *Stroke*, 29(3), pp.705-718.
- [37] Weber, J.T., Rzigalinski, B.A. and Ellis, E.F., 2001. Traumatic injury of cortical neurons causes changes in intracellular calcium stores and capacitative calcium influx. *Journal of Biological Chemistry*, 276(3), pp.1800-1807.
- [38] Ahmadzadeh, H., Smith, D.H. and Shenoy, V.B., 2014. Viscoelasticity of tau proteins leads to strain rate-dependent breaking of microtubules during axonal stretch injury: predictions from a mathematical model. *Biophysical journal*, 106(5), pp.1123-1133.
- [39] Cullen, D.K., Lessing, M.C. and LaPlaca, M.C., 2007. Collagen-dependent neurite outgrowth and response to dynamic deformation in three-dimensional neuronal cultures. *Annals of biomedical engineering*, 35(5), pp.835-846.
- [40] Ellis, E.F., McKinney, J.S., Willoughby, K.A., Liang, S. and Povlishock, J.T., 1995. A new model for rapid stretch-induced injury of cells in culture: characterization of the model using astrocytes. *Journal of neurotrauma*, 12(3), pp.325-339.
- [41] Lusardi, T.A., Rangan, J., Sun, D., Smith, D.H. and Meaney, D.F., 2004. A device to study the initiation and propagation of calcium transients in cultured neurons after mechanical stretch. *Annals of biomedical engineering*, 32(11), pp.1546-1559.
- [42] CARGILL, R.S. and THIBAUT, L.E., 1996. Acute alterations in $[Ca^{2+}]_i$ in NG108-15 cells subjected to high strain rate deformation and chemical hypoxia: an in vitro model for neural trauma. *Journal of neurotrauma*, 13(7), pp.395-407.

- [43] LaPlaca, M.C. and Thibault, L.E., 1997. An in vitro traumatic injury model to examine the response of neurons to a hydrodynamically-induced deformation. *Annals of biomedical engineering*, 25(4), pp.665-677.
- [44] Lusardi, T.A., Wolf, J.A., Putt, M.E., Smith, D.H. and Meaney, D.F., 2004. Effect of acute calcium influx after mechanical stretch injury in vitro on the viability of hippocampal neurons. *Journal of neurotrauma*, 21(1), pp.61-72.
- [45] Rzigalinski, B.A., Weber, J.T., Willoughby, K.A. and Ellis, E.F., 1998. Intracellular free calcium dynamics in stretch-injured astrocytes. *Journal of neurochemistry*, 70(6), pp.2377-2385.
- [46] Maneshi, M.M., Sachs, F. and Hua, S.Z., 2015. A threshold shear force for calcium influx in an astrocyte model of traumatic brain injury. *Journal of neurotrauma*, 32(13), pp.1020-1029.
- [47] Cho, Y., Porto, D.A., Hwang, H., Grundy, L.J., Schafer, W.R. and Lu, H., 2017. Automated and controlled mechanical stimulation and functional imaging in vivo in *C. elegans*. *Lab on a Chip*, 17(15), pp.2609-2618.
- [48] Liu, L., Li, H., Cui, Y., Li, R., Meng, F., Ye, Z. and Zhang, X., 2017. Calcium channel opening rather than the release of ATP causes the apoptosis of osteoblasts induced by overloaded mechanical stimulation. *Cellular Physiology and Biochemistry*, 42(2), pp.441-454.
- [49] Shiwarski, D.J., Darr, M., Telmer, C.A., Bruchez, M.P. and Puthenveedu, M.A., 2017. PI3K class II α regulates δ -opioid receptor export from the trans-Golgi network. *Molecular biology of the cell*, 28(16), pp.2202-2219.
- [50] Fluo Calcium Indicators. (2011). [ebook] ThermoFisher. Available at: <https://www.thermofisher.com/document-connect/document-connect.html?url=https%3A%2F%2Fassets.thermofisher.com%2FTFS->

Assets%2FLSG%2Fmanuals%2Fmp01240.pdf&title=Rmx1byBDYWxjaXVtIEluZGljYXRvcnM= [Accessed 25 Sep. 2019].

Figure 1. 3D in vitro neuron on a chip to probe mechanostimulation. (A) The Nerve Integrated Tissue on Chip approach in the Mechanical Excitation Testbed (MET) system (B) Cellular collagen with PC-12 embedded in it is placed inside a custom acrylic housing ring, which is attached to a coverslip for imaging. The MET system applies a controlled downward force using a voice coil actuator. (C) An image of the system for mechanically stimulating the NITC system with selected frames from a rotation of 3D reconstructed images (500 μm thickness: 0°, 45°, 90°, 180°) captured with confocal microscopy of NGF induced PC-12 cells dispersed through the collagen scaffold labelled with Fluo-4 AM and Deep Red Cell Tracker.

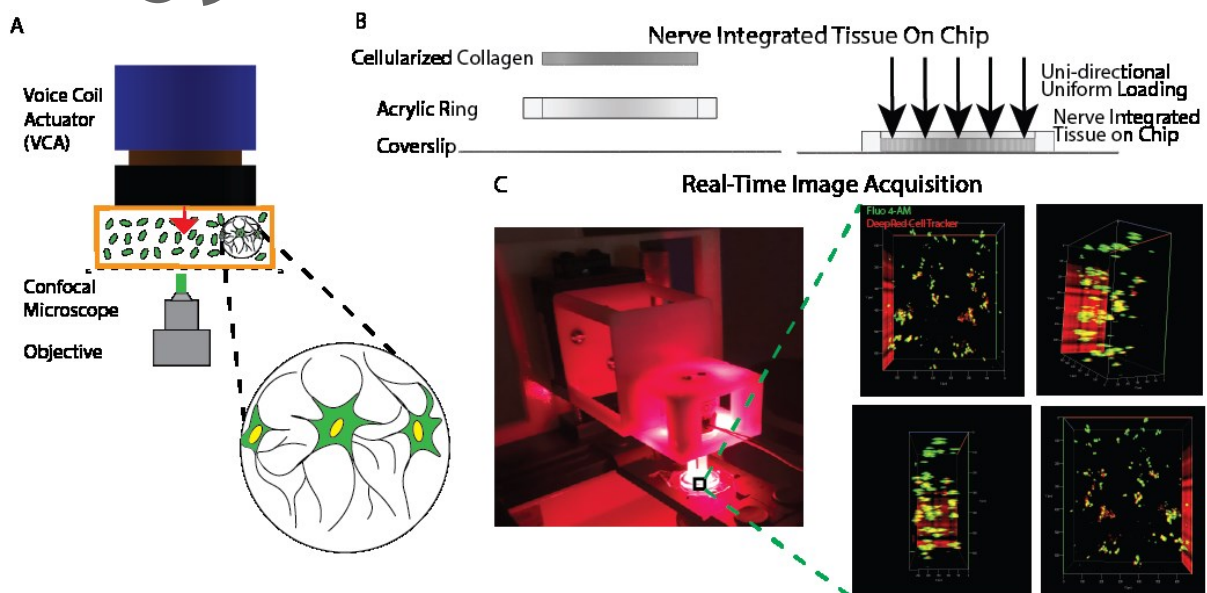


Figure 2. Mechanical Excitation Testbed system for mechanical stimulation of PC-12 cells. (A) Image of the Mechanical Excitation Testbed (MET) system demonstrating the displacement over time functionality of the device. (B) CAD drawing of the MET system consists of a custom 3D printed housing with a voice coil actuator assembly aligned with a spinning disk confocal microscope for real-time imaging. Mounting a z-axis positioner to a 3D printed structural support which is connected to a 2-axis stage allows us to position the precision end effector component for mechanical stimulation of the collagen-cell NITC. A function generator generates a sine waveform is created with (C) a DC-coupled high gain custom electronic voltage amplifier circuit and a single-ended output to smooth the signal for actuating the voice coil actuator with the same waveform and frequency. The end effector actuates to apply compression and enable imaging of cells under mechanical stimulation.

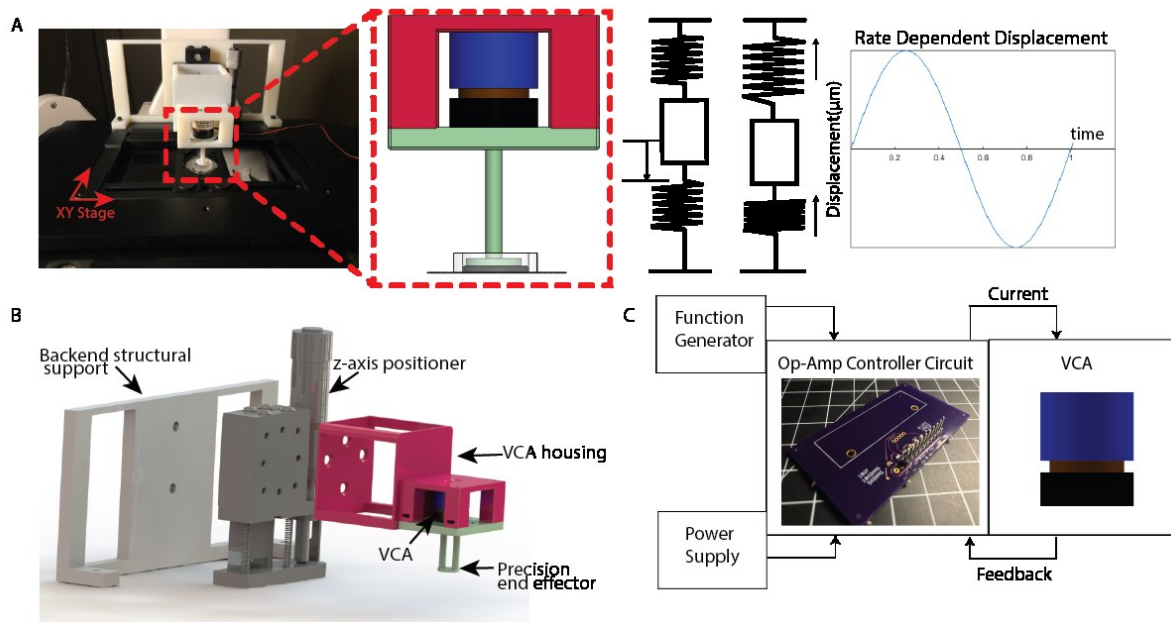


Figure 3. Ca^{2+} response during No-Contact Control phase, Primary phase, and Secondary phase mechanical stimulation in 3D NITC system. Representative schematics of displacement versus time for the mechanical stimulation. Images of the Fluo-4AM labelled differentiated PC-12 cells using spinning disk confocal fluorescent microscopy for (A) No-Contact Control phase, (B) Primary phase, and (C) Secondary phase. Red box indicates areas where cells in the focal plane with Ca^{2+} were analyzed at a strain rate of $\dot{\epsilon} = 4 \times 10^{-2} \text{ s}^{-1}$. Scale bars, 100 μm .

Author

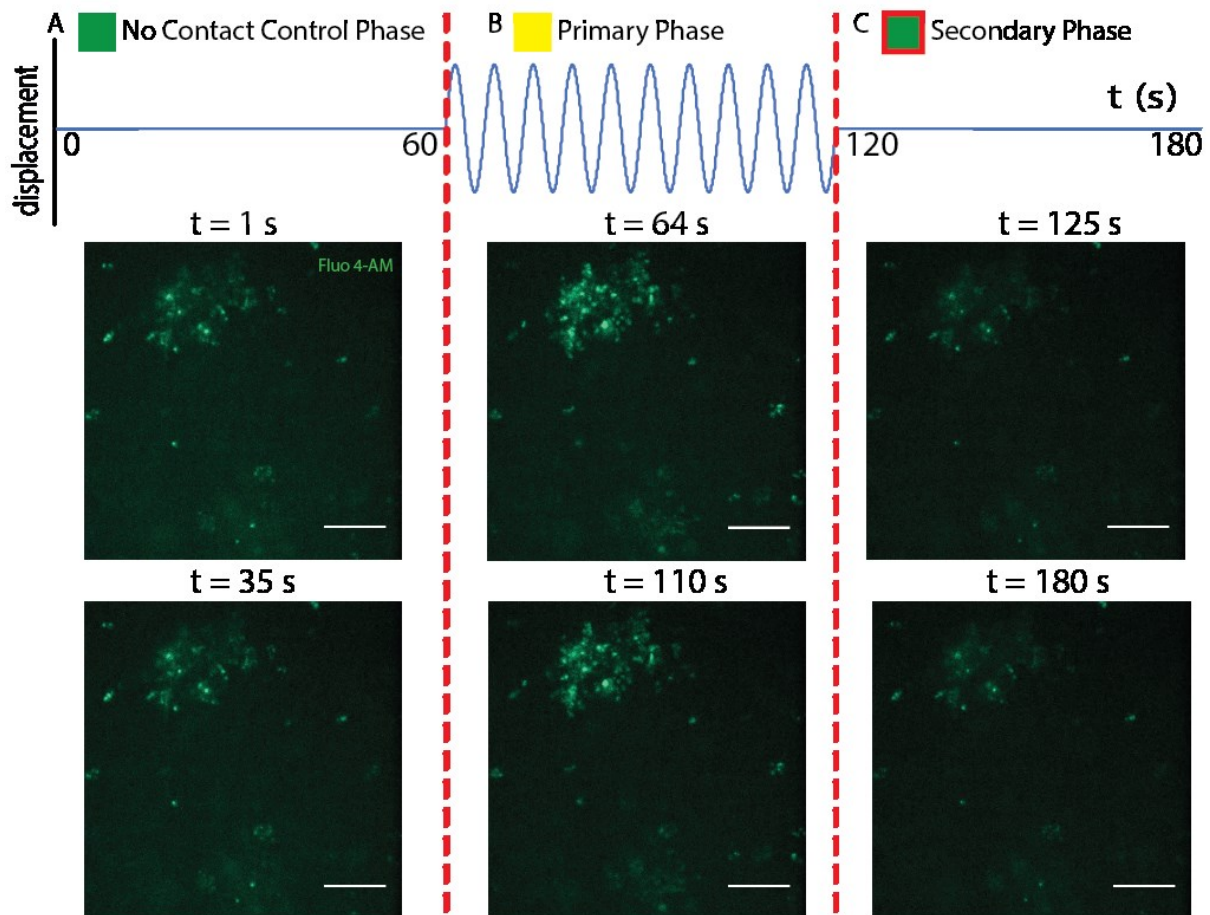
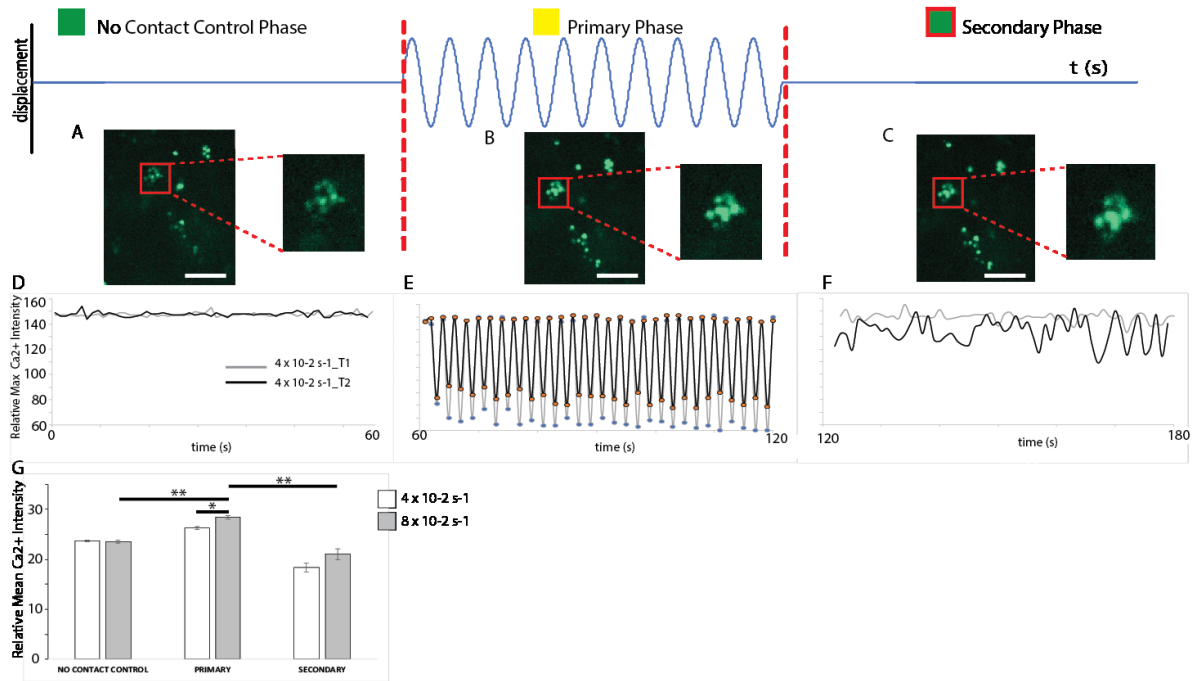


Figure 4. Analysis of Ca^{2+} under mechanical stimulation for the NITC system. (A) Frames from $\dot{\epsilon} = 4 \times 10^{-2} \text{ s}^{-1}$ sample with A) No-contact control phase, B) Primary phase, C) Secondary phase. Scale bars, 50 μm . (D) Quantification of the same strain rate, $\dot{\epsilon} = 4 \times 10^{-2} \text{ s}^{-1}$ at 1 Hz frequency, cell response denoting the No-contact control phase maximum Ca^{2+} intensity values. (T1 and T2 are different representative experiments) (E) Panel denotes maximum Ca^{2+} intensity during the Primary phase. (F) Panel denotes the Secondary phase of maximum Ca^{2+} intensity. (G) Bar graph plot comparing the mean Ca^{2+} ion intensity before, during, and after the Primary phase at strain rates of $\dot{\epsilon} = 4 \times 10^{-2} \text{ s}^{-1}$ (white bar) and $8 \times 10^{-2} \text{ s}^{-1}$ (gray bar). Data presented as mean \pm SD, $n=6$, P-values are calculated using t-test, * $P \leq 0.05$, ** $P \leq 0.01$.

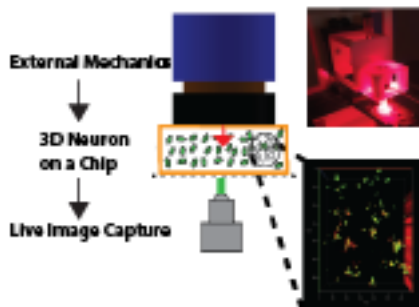


Author Mar

Developing more physiologically relevant 3D neuron integrated systems with external mechanics with synchronized image capture enables understanding of cellular responses that are important for advancing future neural studies and personalized strategies. This work examines calcium response with respect to voice coil actuator controlled force profiles.

J. Bobo*, A. Garg, P. Venkatraman, M. Puthenveedu, P. R. LeDuc*

3D in vitro neuron on a chip for probing calcium mechanostimulation



Author M